

Search for short baseline ν_e disappearance with the T2K near detector

K. Abe,⁴⁷ J. Adam,³³ H. Aihara,^{46,23} T. Akiri,⁹ C. Andreopoulos,⁴⁵ S. Aoki,²⁴ A. Ariga,² S. Assylbekov,⁸ D. Autiero,²⁹ M. Barbi,⁴⁰ G.J. Barker,⁵⁵ G. Barr,³⁶ M. Bass,⁸ M. Batkiewicz,¹³ F. Bay,¹¹ V. Berardi,¹⁸ B.E. Berger,^{8,23} S. Berkman,⁴ S. Bhadra,⁵⁹ F.d.M. Blaszczyk,²⁸ A. Blondel,¹² C. Bojecho,⁵² S. Bordoni,¹⁵ S.B. Boyd,⁵⁵ D. Brailsford,¹⁷ A. Bravar,¹² C. Bronner,²³ N. Buchanan,⁸ R.G. Calland,²⁷ J. Caravaca Rodríguez,¹⁵ S.L. Cartwright,⁴³ R. Castillo,¹⁵ M.G. Catanesi,¹⁸ A. Cervera,¹⁶ D. Cherdack,⁸ G. Christodoulou,²⁷ A. Clifton,⁸ J. Coleman,²⁷ S.J. Coleman,⁷ G. Collazuol,²⁰ K. Connolly,⁵⁶ L. Cremonesi,³⁹ A. Dabrowska,¹³ I. Danko,³⁸ R. Das,⁸ S. Davis,⁵⁶ P. de Perio,⁵⁰ G. De Rosa,¹⁹ T. Dealtry,^{45,36} S.R. Dennis,^{55,45} C. Densham,⁴⁵ D. Dewhurst,³⁶ F. Di Lodovico,³⁹ S. Di Luise,¹¹ O. Drapier,¹⁰ T. Duboyski,³⁹ K. Duffy,³⁶ J. Dumarchez,³⁷ S. Dytman,³⁸ M. Dziewiecki,⁵⁴ S. Emery-Schrenk,⁶ A. Ereditato,² L. Escudero,¹⁶ A.J. Finch,²⁶ G.A. Fiorentini Aguirre,⁵⁹ M. Friend,^{14,*} Y. Fujii,^{14,*} Y. Fukuda,³¹ A.P. Furmanski,⁵⁵ V. Galymov,²⁹ S. Giffin,⁴⁰ C. Giganti,³⁷ K. Gilje,³³ D. Goeldi,² T. Golan,⁵⁸ M. Gonin,¹⁰ N. Grant,²⁶ D. Gudín,²² D.R. Hadley,⁵⁵ L. Haegel,¹² A. Haesler,¹² M.D. Haigh,⁵⁵ P. Hamilton,¹⁷ D. Hansen,³⁸ T. Hara,²⁴ M. Hartz,^{23,51} T. Hasegawa,^{14,*} N.C. Hastings,⁴⁰ T. Hayashino,²⁵ Y. Hayato,^{47,23} C. Hearty,^{4,†} R.L. Helmer,⁵¹ M. Hierholzer,² J. Hignight,³³ A. Hillairet,⁵² A. Himmel,⁹ T. Hiraki,²⁵ S. Hirota,²⁵ J. Holeczek,⁴⁴ S. Horikawa,¹¹ K. Huang,²⁵ A.K. Ichikawa,²⁵ K. Ieki,²⁵ M. Ieva,¹⁵ M. Ikeda,⁴⁷ J. Imber,³³ J. Insler,²⁸ T.J. Irvine,⁴⁸ T. Ishida,^{14,*} T. Ishii,^{14,*} E. Iwai,¹⁴ K. Iwamoto,⁴¹ K. Iyogi,⁴⁷ A. Izmaylov,^{16,22} A. Jacob,³⁶ B. Jamieson,⁵⁷ M. Jiang,²⁵ S. Johnson,⁷ J.H. Jo,³³ P. Jonsson,¹⁷ C.K. Jung,^{33,‡} M. Kabirnezhad,³² A.C. Kaboth,¹⁷ T. Kajita,^{48,‡} H. Kakuno,⁴⁹ J. Kameda,⁴⁷ Y. Kanazawa,⁴⁶ D. Karlen,^{52,51} I. Karpikov,²² T. Katori,³⁹ E. Kearns,^{3,23,‡} M. Khabibullin,²² A. Khotjantsev,²² D. Kielczewska,⁵³ T. Kikawa,²⁵ A. Kilinski,³² J. Kim,⁴ S. King,³⁹ J. Kisiel,⁴⁴ P. Kitching,¹ T. Kobayashi,^{14,*} L. Koch,⁴² A. Kolaceke,⁴⁰ A. Konaka,⁵¹ L.L. Kormos,²⁶ A. Korzenev,¹² Y. Koshio,^{34,‡} W. Kropp,⁵ H. Kubo,²⁵ Y. Kudenko,^{22,§} R. Kurjata,⁵⁴ T. Kutter,²⁸ J. Lagoda,³² I. Lamont,²⁶ E. Larkin,⁵⁵ M. Laveder,²⁰ M. Lawe,⁴³ M. Lazos,²⁷ T. Lindner,⁵¹ C. Lister,⁵⁵ R.P. Litchfield,⁵⁵ A. Longhin,²⁰ L. Ludovici,²¹ L. Magaletti,¹⁸ K. Mahn,³⁰ M. Malek,¹⁷ S. Manly,⁴¹ A.D. Marino,⁷ J. Marteau,²⁹ J.F. Martin,⁵⁰ P. Martins,³⁹ S. Martynenko,²² T. Maruyama,^{14,*} V. Matveev,²² K. Mavrokoridis,²⁷ E. Mazzucato,⁶ M. McCarthy,⁴ N. McCauley,²⁷ K.S. McFarland,⁴¹ C. McGrew,³³ A. Mefodiev,²² C. Metelko,²⁷ M. Mezzetto,²⁰ P. Mijakowski,³² C.A. Miller,⁵¹ A. Minamino,²⁵ O. Mineev,²² A. Missert,⁷ M. Miura,^{47,‡} S. Moriyama,^{47,‡} Th.A. Mueller,¹⁰ A. Murakami,²⁵ M. Murdoch,²⁷ S. Murphy,¹¹ J. Myslik,⁵² T. Nakadaira,^{14,*} M. Nakahata,^{47,23} K. Nakamura,²⁵ K. Nakamura,^{23,14,*} S. Nakayama,^{47,‡} T. Nakaya,^{25,23} K. Nakayoshi,^{14,*} C. Nantais,⁴ C. Nielsen,⁴ M. Nirkko,² K. Nishikawa,^{14,*} Y. Nishimura,⁴⁸ J. Nowak,²⁶ H.M. O’Keeffe,²⁶ R. Ohta,^{14,*} K. Okumura,^{48,23} T. Okusawa,³⁵ W. Oryszczak,⁵³ S.M. Oser,⁴ T. Ovsyannikova,²² R.A. Owen,³⁹ Y. Oyama,^{14,*} V. Palladino,¹⁹ J.L. Palomino,³³ V. Paolone,³⁸ D. Payne,²⁷ O. Perevozchikov,²⁸ J.D. Perkin,⁴³ Y. Petrov,⁴ L. Pickard,⁴³ E.S. Pinzon Guerra,⁵⁹ C. Pistillo,² P. Plonski,⁵⁴ E. Poplawska,³⁹ B. Popov,^{37,¶} M. Posiadala-Zezula,⁵³ J.-M. Poutissou,⁵¹ R. Poutissou,⁵¹ P. Przewlocki,³² B. Quilain,¹⁰ E. Radicioni,¹⁸ P.N. Ratoff,²⁶ M. Ravonel,¹² M.A.M. Rayner,¹² A. Redij,² M. Reeves,²⁶ E. Reinherz-Aronis,⁸ C. Riccio,¹⁹ P.A. Rodrigues,⁴¹ P. Rojas,⁸ E. Rondio,³² S. Roth,⁴² A. Rubbia,¹¹ D. Ruterbories,⁴¹ R. Sacco,³⁹ K. Sakashita,^{14,*} F. Sánchez,¹⁵ F. Sato,¹⁴ E. Scantamburlo,¹² K. Scholberg,^{9,‡} S. Schoppmann,⁴² J. Schwehr,⁸ M. Scott,⁵¹ Y. Seiya,³⁵ T. Sekiguchi,^{14,*} H. Sekiya,^{47,23,‡} D. Sgalaberna,¹¹ F. Shaker,⁵⁷ D. Shaw,²⁶ M. Shiozawa,^{47,23} S. Short,³⁹ Y. Shustrov,²² P. Sinclair,¹⁷ B. Smith,¹⁷ M. Smy,⁵ J.T. Sobczyk,⁵⁸ H. Sobel,^{5,23} M. Sorel,¹⁶ L. Southwell,²⁶ P. Stamoulis,¹⁶ J. Steinmann,⁴² B. Still,³⁹ Y. Suda,⁴⁶ A. Suzuki,²⁴ K. Suzuki,²⁵ S.Y. Suzuki,^{14,*} Y. Suzuki,^{23,23} R. Tacik,^{40,51} M. Tada,^{14,*} S. Takahashi,²⁵ A. Takeda,⁴⁷ Y. Takeuchi,^{24,23} H.K. Tanaka,^{47,‡} H.A. Tanaka,^{4,†} M.M. Tanaka,^{14,*} D. Terhorst,⁴² R. Terri,³⁹ L.F. Thompson,⁴³ A. Thorley,²⁷ S. Tobayama,⁴ W. Toki,⁸ T. Tomura,⁴⁷ Y. Totsuka,^{**} C. Touramanis,²⁷ T. Tsukamoto,^{14,*} M. Tzanov,²⁸ Y. Uchida,¹⁷ A. Vacheret,³⁶ M. Vagins,^{23,5} G. Vasseur,⁶ T. Wachala,¹³ K. Wakamatsu,³⁵ C.W. Walter,^{9,‡} D. Wark,^{45,36} W. Warzycha,⁵³ M.O. Wascko,¹⁷ A. Weber,^{45,36} R. Wendell,^{47,‡} R.J. Wilkes,⁵⁶ M.J. Wilking,³³ C. Wilkinson,⁴³ Z. Williamson,³⁶ J.R. Wilson,³⁹ R.J. Wilson,⁸ T. Wongjirad,⁹ Y. Yamada,^{14,*} K. Yamamoto,³⁵ C. Yanagisawa,^{33,††} T. Yano,²⁴ S. Yen,⁵¹ N. Yershov,²² M. Yokoyama,^{46,‡} K. Yoshida,²⁵ T. Yuan,⁷ M. Yu,⁵⁹ A. Zalewska,¹³ J. Zalipska,³² L. Zambelli,^{14,*} K. Zaremba,⁵⁴ M. Ziembicki,⁵⁴ E.D. Zimmerman,⁷ M. Zito,⁶ and J. Żmuda⁵⁸

(The T2K Collaboration)

¹University of Alberta, Centre for Particle Physics, Department of Physics, Edmonton, Alberta, Canada

²University of Bern, Albert Einstein Center for Fundamental Physics, Laboratory for High Energy Physics (LHEP), Bern, Switzerland

³Boston University, Department of Physics, Boston, Massachusetts, U.S.A.

⁴University of British Columbia, Department of Physics and Astronomy, Vancouver, British Columbia, Canada

⁵University of California, Irvine, Department of Physics and Astronomy, Irvine, California, U.S.A.

- ⁶ IRFU, CEA Saclay, Gif-sur-Yvette, France
- ⁷ University of Colorado at Boulder, Department of Physics, Boulder, Colorado, U.S.A.
- ⁸ Colorado State University, Department of Physics, Fort Collins, Colorado, U.S.A.
- ⁹ Duke University, Department of Physics, Durham, North Carolina, U.S.A.
- ¹⁰ Ecole Polytechnique, IN2P3-CNRS, Laboratoire Leprince-Ringuet, Palaiseau, France
- ¹¹ ETH Zurich, Institute for Particle Physics, Zurich, Switzerland
- ¹² University of Geneva, Section de Physique, DPNC, Geneva, Switzerland
- ¹³ H. Niewodniczanski Institute of Nuclear Physics PAN, Cracow, Poland
- ¹⁴ High Energy Accelerator Research Organization (KEK), Tsukuba, Ibaraki, Japan
- ¹⁵ Institut de Física d'Altes Energies (IFAE), Bellaterra (Barcelona), Spain
- ¹⁶ IFIC (CSIC & University of Valencia), Valencia, Spain
- ¹⁷ Imperial College London, Department of Physics, London, United Kingdom
- ¹⁸ INFN Sezione di Bari and Università e Politecnico di Bari, Dipartimento Interuniversitario di Fisica, Bari, Italy
- ¹⁹ INFN Sezione di Napoli and Università di Napoli, Dipartimento di Fisica, Napoli, Italy
- ²⁰ INFN Sezione di Padova and Università di Padova, Dipartimento di Fisica, Padova, Italy
- ²¹ INFN Sezione di Roma and Università di Roma "La Sapienza", Roma, Italy
- ²² Institute for Nuclear Research of the Russian Academy of Sciences, Moscow, Russia
- ²³ Kavli Institute for the Physics and Mathematics of the Universe (WPI),
Todai Institutes for Advanced Study, University of Tokyo, Kashiwa, Chiba, Japan
- ²⁴ Kobe University, Kobe, Japan
- ²⁵ Kyoto University, Department of Physics, Kyoto, Japan
- ²⁶ Lancaster University, Physics Department, Lancaster, United Kingdom
- ²⁷ University of Liverpool, Department of Physics, Liverpool, United Kingdom
- ²⁸ Louisiana State University, Department of Physics and Astronomy, Baton Rouge, Louisiana, U.S.A.
- ²⁹ Université de Lyon, Université Claude Bernard Lyon 1, IPN Lyon (IN2P3), Villeurbanne, France
- ³⁰ Michigan State University, Department of Physics and Astronomy, East Lansing, Michigan, U.S.A.
- ³¹ Miyagi University of Education, Department of Physics, Sendai, Japan
- ³² National Centre for Nuclear Research, Warsaw, Poland
- ³³ State University of New York at Stony Brook, Department of Physics and Astronomy, Stony Brook, New York, U.S.A.
- ³⁴ Okayama University, Department of Physics, Okayama, Japan
- ³⁵ Osaka City University, Department of Physics, Osaka, Japan
- ³⁶ Oxford University, Department of Physics, Oxford, United Kingdom
- ³⁷ UPMC, Université Paris Diderot, CNRS/IN2P3, Laboratoire de
Physique Nucléaire et de Hautes Energies (LPNHE), Paris, France
- ³⁸ University of Pittsburgh, Department of Physics and Astronomy, Pittsburgh, Pennsylvania, U.S.A.
- ³⁹ Queen Mary University of London, School of Physics and Astronomy, London, United Kingdom
- ⁴⁰ University of Regina, Department of Physics, Regina, Saskatchewan, Canada
- ⁴¹ University of Rochester, Department of Physics and Astronomy, Rochester, New York, U.S.A.
- ⁴² RWTH Aachen University, III. Physikalisches Institut, Aachen, Germany
- ⁴³ University of Sheffield, Department of Physics and Astronomy, Sheffield, United Kingdom
- ⁴⁴ University of Silesia, Institute of Physics, Katowice, Poland
- ⁴⁵ STFC, Rutherford Appleton Laboratory, Harwell Oxford, and Daresbury Laboratory, Warrington, United Kingdom
- ⁴⁶ University of Tokyo, Department of Physics, Tokyo, Japan
- ⁴⁷ University of Tokyo, Institute for Cosmic Ray Research, Kamioka Observatory, Kamioka, Japan
- ⁴⁸ University of Tokyo, Institute for Cosmic Ray Research, Research Center for Cosmic Neutrinos, Kashiwa, Japan
- ⁴⁹ Tokyo Metropolitan University, Department of Physics, Tokyo, Japan
- ⁵⁰ University of Toronto, Department of Physics, Toronto, Ontario, Canada
- ⁵¹ TRIUMF, Vancouver, British Columbia, Canada
- ⁵² University of Victoria, Department of Physics and Astronomy, Victoria, British Columbia, Canada
- ⁵³ University of Warsaw, Faculty of Physics, Warsaw, Poland
- ⁵⁴ Warsaw University of Technology, Institute of Radioelectronics, Warsaw, Poland
- ⁵⁵ University of Warwick, Department of Physics, Coventry, United Kingdom
- ⁵⁶ University of Washington, Department of Physics, Seattle, Washington, U.S.A.
- ⁵⁷ University of Winnipeg, Department of Physics, Winnipeg, Manitoba, Canada
- ⁵⁸ Wrocław University, Faculty of Physics and Astronomy, Wrocław, Poland
- ⁵⁹ York University, Department of Physics and Astronomy, Toronto, Ontario, Canada

(Dated: October 21, 2018)

The T2K experiment has performed a search for ν_e disappearance due to sterile neutrinos using 5.9×10^{20} protons on target for a baseline of 280 m in a neutrino beam peaked at about 500 MeV. A sample of ν_e CC interactions in the off-axis near detector has been selected with a purity of 63% and an efficiency of 26%. The p-value for the null hypothesis is 0.085 and the excluded region at 95% CL is approximately $\sin^2 2\theta_{ee} > 0.3$ for $\Delta m_{\text{eff}}^2 > 7 \text{ eV}^2/\text{c}^4$.

Introduction — In the last two decades, several experiments have observed neutrino oscillations compatible with the hypothesis of neutrino mixing in a three active flavours basis, described by the PMNS matrix [1]. Nevertheless, there exist experimental data that cannot be accommodated in this framework: the deficit of ν_e originating from intense radioactive sources in the calibration of the solar neutrino gallium detectors SAGE [2, 3] and GALLEX [4] and $\bar{\nu}_e$ rates near nuclear reactors [5]. Those experiments cover L/E values of order 1 m/MeV, where L is the neutrino flight-path and E is the neutrino energy, too large to observe any sizeable effect for the standard neutrino mass differences. These anomalies can be interpreted as neutrino oscillations if the PMNS matrix is extended by introducing a new sterile neutrino ν_s (3+1 model) with a mass of order 1 eV/ c^2 [5, 6]. The deficit would be due to $\bar{\nu}_e \rightarrow \nu_s$ oscillations. The ν_e beam component is studied at the ND280 near detectors of the T2K experiment [7] to search for ν_e disappearance. The analysis presented here considers $\nu_e \rightarrow \nu_s$ oscillations, given by the ν_e survival probability in the approximation of two neutrino mass states:

$$P(\bar{\nu}_e \rightarrow \bar{\nu}_e) = 1 - \sin^2 2\theta_{ee} \sin^2 \left(1.267 \frac{\Delta m_{\text{eff}}^2 L}{E} \right) \quad (1)$$

where $\sin^2 2\theta_{ee}$ is the oscillation amplitude, $\Delta m_{\text{eff}}^2 [\text{eV}^2/c^4]$ is the mass squared difference between the new sterile mass state and the weighted average of the active standard mass states, with $L[\text{m}]$ and $E[\text{MeV}]$.

While anomalous excesses that might be explained by $\bar{\nu}_e$ appearance through sterile mixing have been observed by the MiniBooNE [8] and LSND [9] experiments, an explanation of all anomalies as sterile oscillations is disfavoured due to tension between appearance and disappearance data [10–13]. In the absence of a consensus candidate model, new probes using the simple 3+1 model may be able to provide some insights into the existing anomalies. This analysis assumes no ν_μ disappearance or ν_e appearance.

With the given combination of L and E , this analysis is sensitive to ν_e disappearance for $\Delta m_{\text{eff}}^2 \gtrsim 2 \text{eV}^2/c^4$ in a sample of ν_e charged current (CC) interactions [14]. A likelihood ratio fit to the reconstructed neutrino energy spectrum of the ν_e CC interactions is used to test the sterile neutrino hypothesis. A high purity sample of

photon conversions from π^0 decays is included in the fit to control the dominant background in the ν_e sample. In addition, a selection of ν_μ CC interactions at ND280 is used to constrain the neutrino flux and cross section uncertainties in order to substantially reduce the uncertainties on the predicted ν_e CC interaction rate.

The T2K experiment — The T2K experiment uses a neutrino beam produced at the J-PARC facility in Japan to study neutrino oscillations and neutrino interactions [7]. Electron and muon neutrinos are produced from the decay of pions and kaons generated when a 30 GeV proton beam impinges on a graphite target. The detector ND280 sits 280 m from the proton target 2.5° from the primary proton beam direction (off-axis) and observes interactions of neutrinos from the beam, whose ν_e component is peaked at an energy of 500 MeV. The present analysis uses neutrino interactions on polystyrene scintillator or water inside two Fine Grained Detectors (FGDs [15]) that corresponds to a total fiducial mass of about 1.6t. Three Time Projection Chambers (TPCs [16]) adjacent to the FGDs are used to identify particle type and momentum. Electromagnetic calorimeters (ECal [17]) that surround the FGDs/TPCs (the Tracker) along the beam direction (Barrel ECal) and downstream (DsEcal) additionally separate electron showers from muon tracks. The π^0 detector (P0D [18]) is located upstream of the Tracker region and is used to veto interactions outside the FGDs in this analysis.

The results presented in this analysis are based on data taken from January 2010 to May 2013 which corresponds to a total exposure at ND280 of 5.9×10^{20} protons on target (POT) with a horn configuration that enhances neutrinos and suppresses anti-neutrinos.

ν_e flux at ND280 — The T2K beam is composed mostly of ν_μ with 8.8% $\bar{\nu}_\mu$, 1.1% ν_e and 0.1% $\bar{\nu}_e$ [19]. The ν_e flux at ND280 as a function of the neutrino energy is shown in Fig. 1. The fluxes of ν_e and $\bar{\nu}_e$ are produced predominantly by K^\pm and K^0 decays at high energies ($E > 1 \text{ GeV}$), and at low energies ($E < 1 \text{ GeV}$) mainly by μ decay in flight [19]. K^\pm and K^0 tend to decay near the hadron production point due to their short mean lifetime, while μ decay throughout the 96 m long decay volume, with a nearly flat decay length distribution. The ν_e flight path distribution at ND280 is shown in Fig. 2. The average neutrino flight path, for ν_e selected in the analysis, is 244 m. The fluxes at the near detectors are predicted using a full Monte-Carlo simulation of the beam-line and modeling of hadron production cross section based on experimental data from NA61/SHINE [20, 21]. The uncertainties on the ν_e and $\bar{\nu}_e$ fluxes range from 10% to 20% as a function of energy, prior to using any additional information from the ν_μ CC interactions at ND280.

ν interactions at ND280 — The target material of the ν_e CC selection in the Tracker is either water or polystyrene scintillator. At T2K energies, the dominant CC interaction is the CC quasi-elastic (CCQE) scattering off neutrons ($\nu_l n \rightarrow l^- p$), where a negative lepton l^- of the same flavour as the neutrino is created. At higher

* also at J-PARC, Tokai, Japan

† also at Institute of Particle Physics, Canada

‡ affiliated member at Kavli IPMU (WPI), the University of Tokyo, Japan

§ also at Moscow Institute of Physics and Technology and National Research Nuclear University "MEPhI", Moscow, Russia

¶ also at JINR, Dubna, Russia

** deceased

†† also at BMCC/CUNY, Science Department, New York, New York, U.S.A.

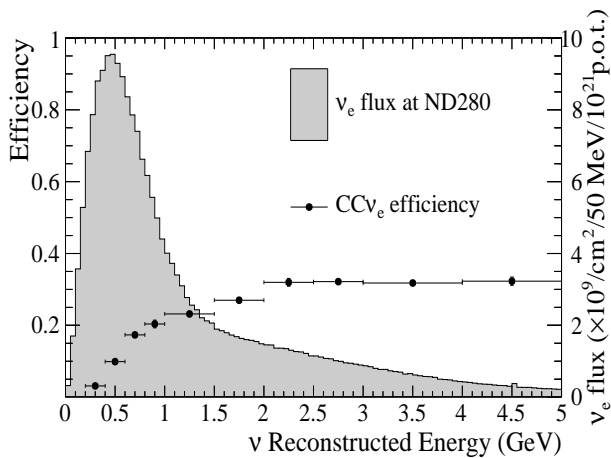


FIG. 1. Expected ν_e flux at ND280 and CC ν_e selection efficiency as a function of the true neutrino energy are shown.

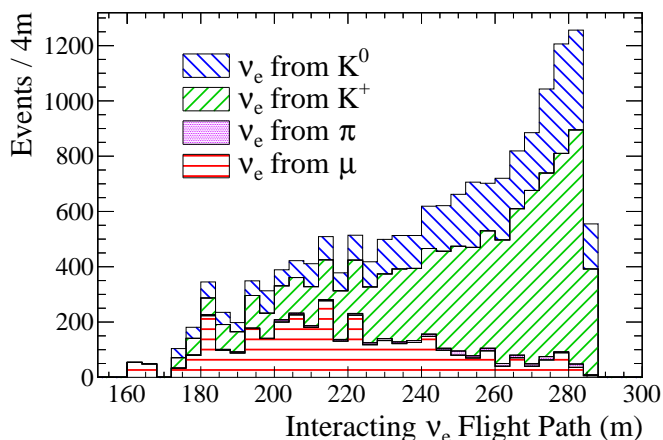


FIG. 2. Expected neutrino flight path for ν_e interacting in the ND280 FV, broken down by the neutrino parent meson.

energies, neutrino CC interactions with pion production can take place. Those are CC resonant single π production (CCRES), coherent π production (CCCoh) and multi- π production due to deep inelastic scattering (CCDIS). As the ν_μ flux is much larger than the ν_e flux, the relative rate of ν_μ CC interactions is expected to be ~ 100 times larger than the analysis signal, ν_e CC interactions. Event selections in the Tracker are designed to enhance the selection of ν -carbon or ν -oxygen interactions inside the FGD fiducial volume (FV).

The most important background for ν_e interactions are $(\bar{\nu}_\mu^-)$ CCDIS or Neutral Current (NC) interactions which produce a π^0 ($\nu_\mu N \rightarrow \pi^0 X$). The π^0 predominantly decays to two photons and any electrons produced within the FV by $\gamma \rightarrow e^+e^-$ may be misidentified as originating from ν_e CC interactions. Electrons in the FV may come from photons produced in ν interactions outside the FV

(OOFV) or inside it.

The neutrino event generator NEUT [22] simulates the neutrino interactions at ND280. Uncertainties in the neutrino-nucleus cross section models and re-interactions of pions within the nucleus (*final state interaction*, FSI) are estimated by comparing the NEUT prediction with external neutrino, pion and electron scattering data [23]. Each cross section is characterized using a minimal set of parameters with large prior uncertainties between 20% and 40%.

Flux and cross section constraints at ND280 — Assuming no ν_μ disappearance, a measurement of ν_μ CC interactions at ND280 is used to reduce the flux and the cross section uncertainties in the ν_e signal prediction. This is possible due to the significant correlation between the ν_μ and ν_e fluxes, originating from decays of the same hadron types. A similar technique is used in other T2K measurements [24, 25]. Possible differences between ν_e and ν_μ cross sections of up to 3%, due to radiative corrections or differences in the nucleon form factors [26], are included as a systematic error.

A predominantly ν_μ CC interaction event sample is selected by identifying the highest momentum negative track originating within the FV which is compatible with a muon. This is done by exploiting the tracking and particle identification capabilities of the TPCs. Based on the presence of charged pions, the ν_μ CC sample is further separated into three categories: events without pions (CC-0 π), events with one π^+ (CC- π^+) and other interactions which produce a π^- , π^0 or more than one pion (CC-Oth). This provides sensitivity to the rate of ν_μ CCQE, CCRES and CCDIS interactions. The three samples are binned in muon momentum and angle and they are fit to evaluate the neutrino flux and cross section uncertainties that are used as prior uncertainties in the ν_e disappearance analysis.

Electron neutrino selection at ND280 and systematic uncertainties — A sample of ν_e CC events is obtained by selecting electron-like events with the most energetic negatively charged track starting either in the FGD1 or FGD2 FV. Electron candidates are selected by combining the particle identification (PID) capabilities of the TPCs and ECals to reject 99.8% of muons. π^0 backgrounds are reduced by rejecting events where a positive electron-like track is identified within 100 mm of the electron candidate and the e^+e^- invariant mass is smaller than 100 MeV/ c^2 . Additionally we require that there are no tracks in the detectors upstream of the interaction vertex to reject $\nu_\mu N \rightarrow \pi^0 X$ interactions outside the FV. ν_e CC interactions are selected with an overall efficiency of 26% (see Fig. 1) and a purity of 63%. The majority of the background (72%) is electrons from conversion of π^0 decay photons ($\nu_\mu N \rightarrow \pi^0 X$). The remaining background is from neutrino interactions where muons (14%) or protons and pions (14%) are misidentified as electrons. A significant component of the background (35%) is due to particles produced outside the FV, as in the magnet, dead materials of the FGDs and TPCs, ECal, P0D or

surrounding material. Those neutrino interactions occur on heavier nuclei (e.g. iron, aluminium, lead) with larger cross section uncertainties (30%). This background is large at low energy.

A control sample is used to measure the $\nu_\mu N \rightarrow \pi^0 X$ background. It is selected by requiring two electron-like tracks in the TPC with a common vertex in the FGD (distance between the starting points of the two tracks less than 10 mm) and invariant mass less than 50 MeV/c². The control sample has an overall selection efficiency with respect to the total number of photons converting in the FGDs of about 12% and is a highly pure background sample predominantly consisting of photon conversion (92%) from $\nu_\mu N \rightarrow \pi^0 X$ in NC and CCDIS interactions. The kinematics of the photons in the control and signal samples are similar. Furthermore, 62% of the control sample ν_μ events are OOFV $\nu_\mu N \rightarrow \pi^0 X$, which provides a direct constraint for the ν_e sample background. A more detailed description of the selection of both the ν_e and the control samples is reported in [14].

The reconstructed ν_e energy spectrum (E_{reco}), assuming a CCQE interaction, is inferred from the outgoing electron candidate momentum and angle, as in [27]. ν_e disappearance would affect the rate and energy spectrum of ν_e CC interactions. Fig. 3 shows the E_{reco} distributions of the ν_e and the control samples. A total of 614 ν_e CC candidates are selected in the ν_e sample and 665 ± 51 (syst) events are expected, assuming no oscillation and with the systematic uncertainties described below. The number of selected events in the control sample is 989 in data, with an expectation of 1236 ± 246 (syst). Systematic uncertainties on the flux, cross section and detector response are taken into account using the approach adopted in [14]. The systematic uncertainties on the flux and ν_e - ν_μ common cross sections are constrained by fitting the ν_μ CC sample as described earlier. The unconstrained cross-section systematic uncertainties include several contributions: the difference between the interaction cross section of ν_μ and ν_e , between ν and $\bar{\nu}$ and the uncertainty on OOFV interactions. FSI uncertainties contribute 1.5% (2.7%) to the ν_e ($\nu_\mu N \rightarrow \pi^0 X$) sample systematic uncertainty. The detector systematic uncertainties have been evaluated independently for the TPCs, FGDs and ECal. The largest sources of uncertainties are given by the TPC momentum resolution and the PID. In Table I, the effect of each group of systematic uncertainties on the total expected number of signal and signal plus background events is shown. In Fig. 3 the effect of the systematic uncertainties on the E_{reco} distributions is shown. The simulation overestimates the data in both the ν_e and control sample distributions at low energy. However this overestimation in the control sample is within one standard deviation of expectation.

Oscillation fit — The sterile oscillation parameters $\sin^2 2\theta_{ee}$ and Δm_{eff}^2 are estimated with a Poisson binned likelihood ratio method. The expected reconstructed neutrino energy distributions are compared to data with a simultaneous fit to the selected ν_e and control samples.

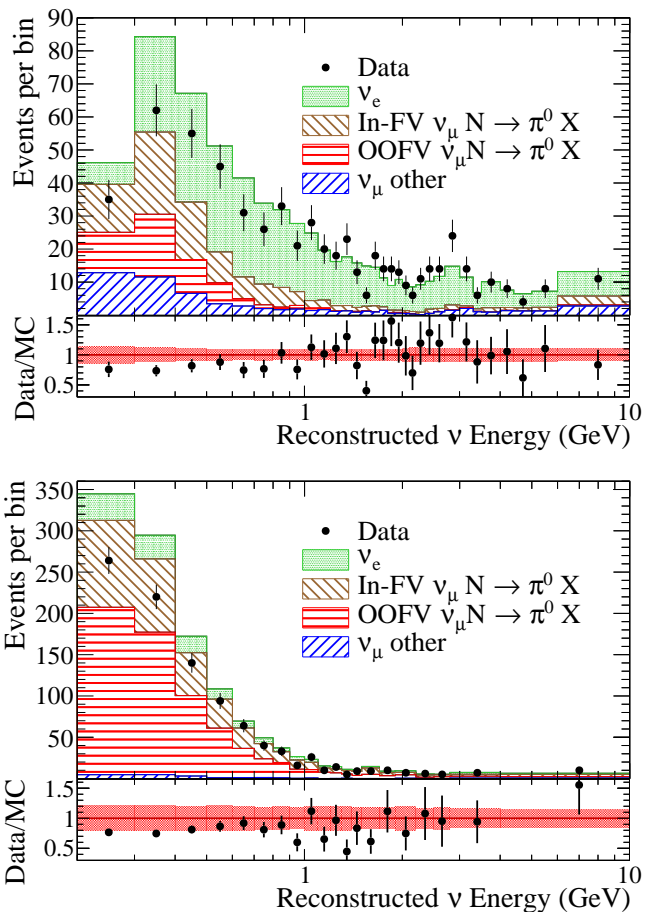


FIG. 3. Reconstructed energy distributions of the ν_e (top) and control (bottom) samples. The distributions are broken down by ν_e interactions (signal), background inside the fiducial volume due to $\nu_\mu N \rightarrow \pi^0 X$ (In-FV $\nu_\mu N \rightarrow \pi^0 X$), background outside the fiducial volume due to $\nu_\mu N \rightarrow \pi^0 X$ (OOFV $\nu_\mu N \rightarrow \pi^0 X$) and all other sources of background (ν_μ other). Both ν and $\bar{\nu}$ are included in the samples. The ratio of the data to the MC expectation in the null oscillation hypothesis is shown for both samples. The red error band corresponds to the fractional systematic uncertainty. Black dots represent the data with the statistical uncertainty.

TABLE I. Fractional variation (RMS/mean in %) of the expected total number of events for ν_e (all events and signal only) and control sample in the null oscillation hypothesis due to the effect of the systematic uncertainties. Existing correlations between systematics are taken into account.

Error source (# param.)	ν_e sample (sig+bkg)	ν_e sample (sig only)	control sample
$\nu_\mu - \nu_e$ common (40)	4.4	5.2	6.7
Unconstrained (5)	3.7	3.0	17.8
Detector + FSI (10)	5.1	5.5	5.5
Total (55)	7.6	8.1	19.9

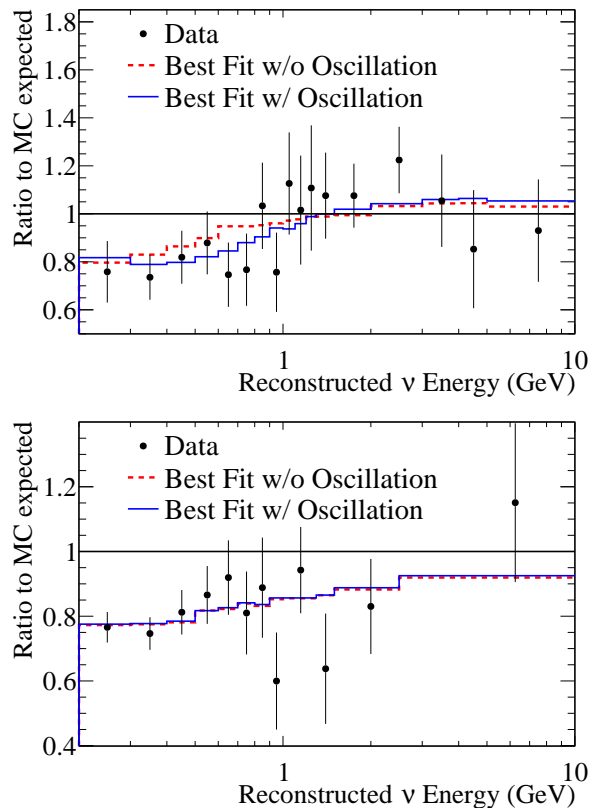


FIG. 4. The ratio of the best fit spectrum to the expected MC distribution, where the fit includes nuisance and oscillation parameters (blue) and nuisance parameters only (red dashed), is shown. The plots show the ν_e sample (top) and the control sample (bottom). The black line corresponds to the expected non-oscillated MC before the fit. The black dots show the data. Statistical uncertainties are shown.

The range of E_{reco} is from 0.2 GeV to 10 GeV. The oscillation amplitude $\sin^2 2\theta_{ee}$ is restricted to the physical region. The effect of systematic uncertainties is included in the fit with nuisance parameters (55 in total) constrained by a Gaussian penalty term. The oscillation probability Eq. (1) affects ν_e signal events based on the true neutrino energy and flight path.

The best-fit oscillation parameters are $\sin^2 2\theta_{ee} = 1$ and $\Delta m_{eff}^2 = 2.05 \text{ eV}^2/c^4$. The χ^2/ndf is 42.16/49. Most of the best-fit systematic parameters are within a 0.5σ deviations and always within 1σ from the prior values. The systematic parameter corresponding to the normalization of the $\nu_\mu N \rightarrow \pi^0 X$ OOFV component is reduced by 31% ($\sim 1\sigma$) due to the deficit at low energy in the control sample. The ratio between the best-fit and the expected non-oscillated MC distributions is shown as a function of E_{reco} for both the ν_e and the control samples in Fig. 4. The best-fit, where the nuisance parameters are allowed to float while the oscillation parameters are fixed to null, is also shown. The corresponding χ^2/ndf is 45.86/51.

The two-dimensional confidence intervals in the $\sin^2 2\theta_{ee} - \Delta m_{eff}^2$ parameter space are computed using

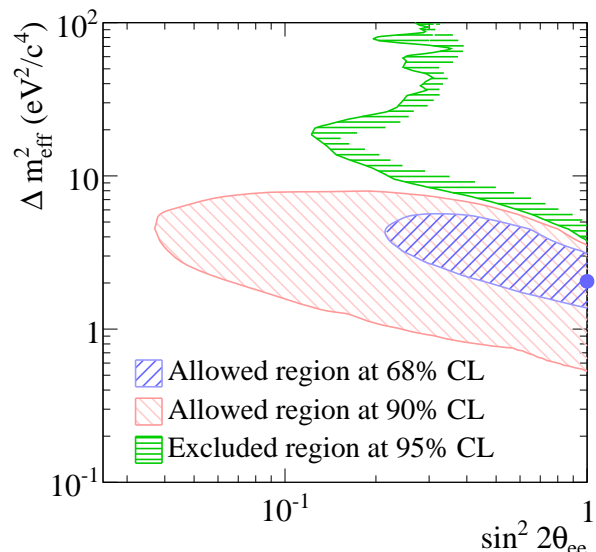


FIG. 5. 68% and 90% CL allowed regions and 95% CL exclusion region for the $\sin^2 2\theta_{ee} - \Delta m_{eff}^2$ parameters measured with the T2K near detector.

the Feldman-Cousins method [28]. The systematic uncertainties are incorporated using the method described in [29]. The 68%, 90% and 95% confidence regions are shown in Fig. 5. The exclusion region at 95% CL is approximately given by $\sin^2 2\theta_{ee} > 0.3$ and $\Delta m_{eff}^2 > 7 \text{ eV}^2/c^4$.

The p -value of the null oscillation hypothesis, computed using a profile likelihood ratio as a test statistic, is 0.085.

The impact of ν_μ disappearance and ν_e appearance on the present result is estimated by considering a non-null $\sin^2 2\theta_{\mu\mu}$ in the 3+1 model. For $\sin^2 2\theta_{\mu\mu}$ between 0 and 0.05, approximately the region not excluded by other experiments [10, 30], the 95%CL exclusion on $\sin^2 2\theta_{ee}$ moves by less than 0.1

In Fig. 6 the T2K excluded region at 95% CL is compared with ν_e disappearance allowed regions from the gallium anomaly and reactor anomaly. The excluded regions from $\nu_e + {}^{12}\text{C} \rightarrow {}^{12}\text{N} + e^-$ scattering data of KARMEN [31, 32] and LSND [33] experiments and solar neutrino and KamLAND data [34–46] are also shown. The T2K result excludes part of the gallium anomaly and a small part of the reactor anomaly allowed regions. The current T2K limit at 95% CL is contained within the region excluded by the combined fit of the solar and KamLAND data.

Conclusions — T2K has performed a search for ν_e disappearance with the near detector. The excluded region at 95% CL is approximately $\sin^2 2\theta_{ee} > 0.3$ and $\Delta m_{eff}^2 > 7 \text{ eV}^2/c^4$. The p -value of the null oscillation hypothesis is 0.085. Further data from T2K will reduce the statistical uncertainty, which is still an important limitation for the analysis.

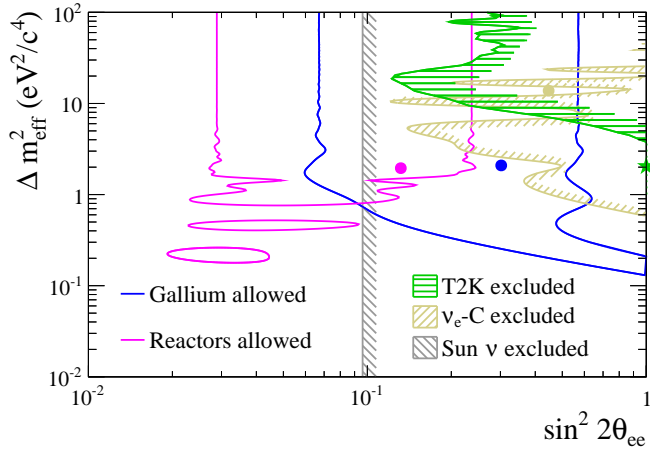


FIG. 6. The T2K excluded region in the $\sin^2 2\theta_{ee} - \Delta m_{\text{eff}}^2$ parameter space at 95% CL is compared with the other experimental results available in literature: allowed regions of gallium and reactor anomalies and excluded regions by ν_e -carbon interaction data and solar neutrino data [13]. The T2K best fit is marked by a green star; the best fit of other experimental results corresponds to circles of the same coloring as the limits.

We thank the J-PARC staff for superb accelerator performance and the CERN NA61 collaboration for providing valuable particle production data. We acknowledge the support of MEXT, Japan; NSERC, NRC and CFI, Canada; CEA and CNRS/IN2P3, France; DFG, Germany; INFN, Italy; National Science Centre (NCN), Poland; RSF, RFBR and MES, Russia; MINECO and ERDF funds, Spain; SNSF and SER, Switzerland; STFC, UK; and DOE, USA. We also thank CERN for the UA1/NOMAD magnet, DESY for the HERA-B magnet mover system, NII for SINET4, the WestGrid and SciNet consortia in Compute Canada, GridPP, UK. In addition participation of individual researchers and institutions has been further supported by funds from: ERC (FP7), EU; JSPS, Japan; Royal Society, UK; DOE Early Career program, USA.

-
- [1] Z. Maki and M. Nakagawa and S. Sakata, Prog. Theor. Phys. **28**, 870 (1962).
- [2] J. N. Abdurashitov *et al.* (SAGE collaboration), Phys. Rev. C **59**, 2246 (1999).
- [3] J. N. Abdurashitov *et al.* (SAGE collaboration), Phys. Rev. C **73**, 045805 (2006).
- [4] F. Kaether *et al.*, Phys. Lett. B **685**, 073006 (2010).
- [5] G. Mention *et al.*, Phys. Rev. D **83**, 073006 (2011).
- [6] M. A. Acero *et al.*, Phys. Rev. D **78**, 073009 (2008).
- [7] K. Abe *et al.* (T2K Collaboration), Nucl. Instrum. Meth. **A659**, 106, (2011).
- [8] Aguilar-Arevalo *et al.* (MiniBooNE Collaboration), Phys. Rev. Lett. **105**, 181801 (2010).
- [9] Aguilar-Arevalo *et al.* (LSND Collaboration), Phys. Rev. D **64**, 112007 (2001).
- [10] J. Kopp *et al.*, JHEP **1305**, 050 (2013).
- [11] J. M. Conrad *et al.*, arXiv:1207.4765 [hep-ex] (2012).
- [12] C. Giunti *et al.*, Phys. Rev. D **88**, 073008 (2013).
- [13] C. Giunti *et al.*, Phys. Rev. D **86**, 113014 (2012).
- [14] K. Abe *et al.* (T2K Collaboration), Phys. Rev. D **89**, 092003 (2014).
- [15] P. Amaudruz *et al.*, Nucl. Instrum. Methods **A696**, 1 (2012).
- [16] N. Abgrall *et al.*, Nucl. Instrum. Methods **A637**, 25 (2011).
- [17] D. Allan, *et al.*, JINST, **8**, P10019 (2013).
- [18] S. Assylbekov *et al.*, Nucl. Instrum. Methods **A686**, 48 (2012).
- [19] K. Abe *et al.* (T2K Collaboration), Phys. Rev. D **87**, 012001 (2013).
- [20] N. Abgrall *et al.* (NA61/SHINE Collaboration), Phys. Rev. C **84**, 034604, (2011).
- [21] N. Abgrall *et al.* (NA61/SHINE Collaboration), Phys. Rev. C **85**, 035210 (2012).
- [22] Y. Hayato, Phys. Proc. Supp. **B112**, 171 (2002).
- [23] K. Abe *et al.* (T2K Collaboration), Phys. Rev. D **88**, 032002 (2013).
- [24] K. Abe *et al.* (T2K Collaboration), Phys. Rev. Lett. **112**, 061802 (2014).
- [25] K. Abe *et al.* (T2K Collaboration), Phys. Rev. Lett. **112**, 092003 (2014).
- [26] M. Day and K.S. McFarland, Phys. Rev. D **86**, 053003 (2012).
- [27] K. Abe *et al.* (T2K Collaboration), Phys. Rev. Lett. **111**, 211803 (2013).
- [28] G. J. Feldman and R. D. Cousins, Phys. Rev. D **57**, 3873 (1998).
- [29] J. Stuart, A. Ord and S. Arnold, Kendall's Advanced Theory of Statistics, Vol 2A (6th Ed.) (Oxford University Press, New York, 1994).
- [30] Cheng, G. *et al.* (MiniBooNE and SciBooNE Collaborations), Phys. Rev. D **86**, 052009 (2012).
- [31] B.E. Bodmann *et al.* (KARMEN Collaboration), Phys. Lett. B **332**, 251 (1994).
- [32] B. Armbruster *et al.*, Phys. Rev. C **57**, 3414 (1998).
- [33] L. B. Auerbach *et al.* (LSND Collaboration), Phys. Rev. C **64**, 065501 (2001).
- [34] F. Kaether, W. Hampel, G. Heusser, J. Kiko, and T. Kirsten, Phys. Lett. B **685**, 47 (2010).
- [35] B. T. Cleveland *et al.* (Homestake Collaboration), Astrophys. J. **496**, 505 (1998).
- [36] J.N. Abdurashitov *et al.* (SAGE Collaboration), J. Exp. Theor. Phys. **95**, 181 (2002).
- [37] J. Hosaka *et al.* (Super-Kamkiokande Collaboration), Phys. Rev. D **73**, 112001 (2006).
- [38] J. Cravens *et al.* (Super-Kamkiokande Collaboration), Phys. Rev. D **78**, 032002 (2008).
- [39] K. Abe *et al.* (Super-Kamkiokande Collaboration),

- Phys.Rev. D **83**, 052010 (2011).
- [40] M. Smy (Super-Kamiokande Collaboration), in XXV International Conference on Neutrino Physics and Astrophysics, 2012 (Neutrino, Kyoto, 2012).
- [41] Q. R. Ahmad *et al.* (SNO Collaboration), Phys. Rev. Lett. **89**, 011302 (2002).
- [42] B. Aharmim *et al.* (SNO Collaboration), Phys. Rev. C **72**, 055502 (2005).
- [43] B. Aharmim *et al.* (SNO Collaboration), Phys. Rev. Lett. **101**, 111301 (2008).
- [44] G. Bellini *et al.* (Borexino Collaboration), Phys. Rev. Lett. **107**, 141302 (2011).
- [45] G. Bellini *et al.* (Borexino Collaboration), Phys. Rev. Lett. **108**, 051302 (2012).
- [46] A. Gando *et al.* (KamLAND Collaboration), Phys. Rev. D **83**, 052002 (2011).